Published in final edited form as:
Cancer Cell. 2008 August 12; 14(2): 123–134. doi:10.1016/j.ccr.2008.07.005.

Acquisition of granule neuron precursor identity is a critical determinant of progenitor cell competence to form Hedgehog-induced medulloblastoma

Ulrich Schüller[1,10,*], **Vivi M. Heine**[1,2,3,*], **Junhao Mao**[4], **Alvin T. Kho**[5], **Allison K. Dillon**[2,3], **Young-Goo Han**[3], **Emmanuelle Huillard**[2,3], **Tao Sun**[1], **Azra H. Ligon**[1,8], **Ying Qian**[1], **Qiufu Ma**[1], **Arturo Alvarez-Buylla**[3,6], **Andrew P. McMahon**[4], **David H. Rowitch**[1,2,3,6,7,§], and **Keith L. Ligon**[1,8,9,§]

1*Dana-Farber Cancer Institute, Harvard Medical School, 44 Binney Street, Boston, MA 02115*

2*Howard Hughes Medical Institute, UCSF, 513 Parnassus Avenue, San Francisco CA 94143*

3*Institute for Regeneration Medicine, UCSF, 513 Parnassus Avenue, San Francisco CA 94143*

4*Dept. of Molecular and Cellular Biology, Harvard University, 16 Divinity Avenue, Cambridge, MA 02138*

5*Informatics Program, Children's Hospital, 300 Longwood Avenue, Boston, MA 02115*

6*Dept. of Neurological Surgery, UCSF, 505 Parnassus Avenue, San Francisco, CA 94143*

7*Dept. of Pediatrics, UCSF, 505 Parnassus Avenue, San Francisco, CA 94143*

8*Dept. of Pathology, Brigham and Women's Hospital, 75 Francis Street*

9*Center for Molecular Oncologic Pathology, Dana-Farber Cancer Institute, and Dept. of Pathology, Children's Hospital, Boston, MA 02115.*

10*Center for Neuropathology, Ludwig-Maximilians-Universität, Feodor-Lynen-Strasse 23, 81377 Munich, Germany.*

Abstract

Origins of the brain tumor, medulloblastoma, from stem cells or restricted progenitor cells are unclear. To investigate this, we activated oncogenic Hedgehog (Hh) signaling in multipotent and lineage-restricted CNS progenitors. We observed that normal unipotent cerebellar granule neuron precursors (CGNP) derive from *hGFAP*$^+$ and *Olig2*$^+$ RL progenitors. Hh activation in a spectrum of early and late stage CNS progenitors generated similar medulloblastomas, but not other brain cancers, indicating that acquisition of CGNP identity is essential for tumorigenesis. We show in human and mouse medulloblastoma that cells expressing the glia-associated markers Gfap and Olig2 are neoplastic and that they retain features of embryonic-type granule lineage progenitors. Thus, oncogenic Hh signaling promotes medulloblastoma from lineage-restricted granule cell progenitors.

*These authors contributed equally.
§Authors for correspondence: rowitchd@peds.ucsf.edu; keith_ligon@dfci.harvard.edu

Significance

Cancer stem cells have been proposed as therapeutic targets in human brain cancer. Although such populations have been reported in medulloblastoma, tumor progenitor origins remain unclear. Here we show that medulloblastoma (MB) is generated from cells related to several stages of cerebellar granule neuron precursor (CGNP) development, and that some tumor cells, demonstrable in murine models and human MB, retain primitive features analogous to precursors of the embryonic brain. These data highlight the importance of a developmental perspective in understanding cells involved in CNS tumor progression and the histopathological composition of brain cancers. They suggest that a potential therapeutic target is the process regulating acquisition of CGNP phenotype.

Introduction

It has been proposed that cancer can be viewed as aberrant organogenesis initiated by a multipotent or restricted progenitor cell that acquires infinite capacity for self-renewal through accumulated mutations (Reya et al., 2001). Principles of normal hematopoietic stem cell development (Barabe et al., 2007; Cobaleda et al., 2007) have provided insight into the mechanisms of self-renewal and multi-lineage differentiation in hematopoietic malignancies (Faber and Armstrong, 2007; Warner et al., 2004). However, for most organ systems parallels between normal stem cell development and solid tumor formation remain poorly understood.

The central nervous system (CNS), with its highly diversified classes of neuronal and glial progenitor cells, provides a suitable model to study such mechanisms. Several studies have documented the existence of cancer stem cells for glioma and the cerebellar tumor, medulloblastoma (MB) with properties reminiscent of normal neural precursors (Singh et al., 2004; Galli et al., 2004; Hemmati et al., 2003). Expression profiling has indicated correlations between specific stages of cerebellar development and MB (Lee et al., 2003; Kho et al., 2004). The Sonic hedgehog (Shh) pathway has critical functions in cerebellar development and mutations of pathway are etiologic in MB (Pietsch et al., 1997).

The cerebellum (CB) develops from several progenitor regions: the rostral rhombic lip (rRL) and cells of the ventricular zone (VZ) surrounding the IVth ventricle (Altmann and Bayer, 1997; Morales and Hatten, 2006; Kawauchi et al., 2006; Casper and McCarthy, 2006; Malatesta et al., 2003) (Figure 1A). The VZ of the cerebellar anlage generates Purkinje neurons (PN), interneurons (IN), and glia cells. Progenitors within the rRL express the radial glial markers, RC2 and Nestin, and give rise to all granule lineage cells (GC) of the EGL and IGL. We recently reported that cells which express cre recombinase under control of human regulatory sequences for *Glial Fibrillary Acidic Protein* (*hGFAP*), are most probably radial glia and generate most cerebellar cell types including CGNP (Spassky et al., 2008). Subsequently, CGNP migrate rostrally along the surface of the cerebellar anlagen to form the external granule layer (EGL) (Lee et al., 2005; Machold and Fishell, 2005; Wang et al., 2005) (Figure 1A).

PN (Figure 1B) produce Shh, which binds the transmembrane protein repressor Patched (Ptc), relieving inhibition of Smoothened (Smo) activity, which is essential for CGNP proliferation in the EGL (Wechsler-Reya and Scott, 1999; Dahmane and Altaba, 1999; Lewis et al., 2004). CGNP of the EGL gradually show reduced proliferation levels, migrate internally and differentiate into glutamatergic neurons in the internal granule layer (IGL) (Figure 1B), a process that is largely completed by postnatal day 15 (P15) in mice (Borghesani et al., 2002), and by about a year of age in the human CB (Abraham et al., 2001). Transcriptional control of CGNP development involves functions of bHLH protein Math1 (Ben Arie et al., 1997; Machold and Fishell, 2005; Wang et al., 2005), and homeodomain protein Pax6 (Engelkamp et al., 1999; Yamasaki et al., 2001).

Inherited activating mutations of the Shh-Smo pathway in humans are etiologic in MB but not glioma (Hahn et al., 1999; Johnson et al., 1996). This cancer spectrum is faithfully modeled in the CNS of mice heterozygous for a mutation of the Hedgehog (Hh) pathway suppressor *Ptc1* (Johnson et al., 1996) or expressing an activated allele of *Smoothened* (*SmoM2*) (Mao et al., 2006), supporting the proposal that CGNP are particularly susceptible to transformation by oncogenic Hh signaling (Shih and Holland, 2004). Nevertheless, the cellular origins of MB from unipotent precursors in the EGL remain controversial. The identification of multipotent MB stem cells (Hemmati et al., 2003; Singh et al., 2004) capable of multi-lineage differentiation, in particular, has challenged the hypothesis of a unipotent cell-of-origin. To investigate these issues, we defined distinct progenitor populations for CGNP within the rRL as well as in the EGL and systematically assessed their tumorigenic potential with respect to Hh signaling.

Results

Olig2 expression identifies RL progenitors for a subset of granule cell neurons

In order to determine possible parallels between progenitors during cerebellar development and tumorigenesis, we first characterized relevant embryonic hindbrain VZ and RL populations. Nuclei of cells that express cre proteins in *hGFAP-cre* mice are observed along the VZ and the ventral aspect of the rRL of the midline cerebellar anlage at E14.5 (Figure 1C-E). Cre proteins in these mice mark nestin^{+} cells that have been proposed to be radial glia of the rRL that give rise to CGNP (Spassky et al., 2008), which show robust Pax6 expression. We next investigated expression of the bHLH protein, Olig2, which marks multilineage progenitor populations of the forebrain and the spinal cord (Petryniak et al., 2007; Lu et al., 2002; Zhou and Anderson, 2002). Olig2 expression identified a distinct cell population predominantly restricted to the rRL and extending to the boundary of the EGL (Figure 1F). The cerebellar VZ contained rare Olig2^{+} cells and expression of Olig2 was rapidly down regulated within the EGL.

To establish a possible lineage relationship between *hGFAP-cre* and Olig2^{+} cells, we fate mapped *hGFAP-cre*-expressing precursors with a conditional *ROSA26-eYPF*$^{Fl/Fl}$ reporter (Srinivas et al., 2001). As shown (Figure 1G, white line), *hGFAP-cre*-expressing precursors give rise to the majority of CGNP of the primitive EGL, and some Olig2^{+} cells of the rRL (Figure 1H). Most Olig2^{+} cells in the rRL co-expressed the CGNP marker, Pax6 (Figure 1I) while Olig2 expression was gradually lost and Pax6 retained as CGNP migrated into the EGL. Olig2^{+}Pax6^{+} cells could be identified within the rRL and EGL until E18.5, but were never observed at P7 or later stages (data not shown; Figure 6E,F).

To establish Olig2^{+} progenitor contributions during CGNP development, we constructed a multi-functional mouse line by inserting *tva*, an avian-specific retroviral receptor, and an *IRES-cre* recombinase cassette into the endogenous *Olig2* locus by homologous recombination (Figure 2A). When *Olig2-tva-cre*$^{+/-}$ mice were crossed to *ROSA26-eYFP*$^{Fl/Fl}$ conditional reporter mice, we found that 98% of YFP^{+} cells in the P7 cerebellar white matter (WM) expressed Olig2, consistent with oligodendroglial identity (Figure 2B, C, yellow arrows). At P21 most of these cells co-expressed myelin basic protein, and we observed small numbers of YFP^{+} PN and IN (Supp. Figure 1E, F). At P7, we detected a small subpopulation of YFP^{+} CGNP within the EGL, confined mainly to posterior cerebellar Lobes IX/X (Figure 2C-E, white arrows). At P21, we observed fate mapping to GC within the IGL (Figure 2F-I). Interestingly, only 3% of YFP^{+} cells expressed the GC marker Zic in the Lobe II IGL, but 58% of YFP^{+} cells were double positive in Lobe X (Figure 2G and I), indicating that Olig2 contributions to GC of the IGL are restricted mainly to the posterior lobes.

We found Olig2$^+$ cells in the rRL from E14.5-18.5 (Figure 1 and data not shown). To test whether these cells in particular were a source of lobe IX-X CGNP, we injected the rRL of E15.5 *Olig2-tva-cre*$^{+/-}$ animals with an avian retrovirus (RCAS-GFP), which can only transduce *tva*-expressing cells (Figure 2J). Fate mapping results analyzed at P7 indicated that infected rRL *Olig2-tva*$^+$ cells generate Pax6$^+$ CGNP of the EGL and Zic$^+$ GC within the IGL (Figure 2K-M, Suppl. Figure 1) of lobes IX and X. Taken together, these data indicate that *Olig2*$^+$ progenitors of the rRL make restricted contributions to the GC lineage, particularly in posterior lobes of the CB.

Smoothened activation within CNS *hGFAP*$^+$ and *Olig2*$^+$ progenitors produces only medulloblastoma

To determine the significance of *hGFAP*- and *Olig2*-expressing progenitor populations for CNS tumorigenesis, we used *hGFAP-cre* and *Olig2-tva-cre* drivers, respectively, to conditionally express an activated *Smo (SmoM2)* allele fused with *yellow fluorescent protein (YFP)* sequences (Mao et al., 2006). All *hGFAP-cre:SmoM2* mice developed diffuse tumors with the characteristic “small round blue cell” histology of MB (Figure 3A-D, Table 1). *Olig2-tva-cre:SmoM2* mice developed tumors with similar histology, except that they were focal, localized to the posterior-lateral lobes and had significantly (p <0.01) later mortality (Figure 3E-H, Table 1), which was likely a result of their focal nature and the small numbers of CGNP targeted by *Olig2-tva-cre*.

Although hGFAP$^+$ and Olig2$^+$ progenitor populations give rise, collectively, to CGNP as well as IN, astrocytes (AS) and oligodendrocytes (OL), we only observed cerebellar tumors with histological features of MB. Additionally, activated Hh signaling in cerebellar PN driven by *Shh-creERT2* never resulted in MB (Table 1). These data demonstrate that *hGFAP*$^+$ and *Olig2*$^+$ multipotent progenitor populations can produce MB.

Hh signaling can have mitogenic effects in spinal cord and forebrain (Mao et al., 2006; Rowitch et al., 1999; Fuccillo et al., 2006), and roles in forebrain glioma have been reported (Clement et al., 2007; Ehtesham et al., 2007). However, no evidence of gliomas or other primitive neuroectodermal tumors (PNET) in the forebrain was observed despite forced expression of SmoM2 in the subventricular zone, in NG2$^+$ progenitors, and in oligodendrocyte precursor cells (OPC) of the forebrain (Table 1, Figure 3I-L). Together, these data indicate a hindbrain- as well as a CGNP/lineage-restricted oncogenic response to Hh signaling, and raised the question of whether this was determined by the particular environmental niche of the EGL. To assess this, we transplanted freshly dissociated cells from *Olig2-tva-cre:SmoM2* tumors into the forebrains and cerebella of SCID mice. Because tumors formed equally well in both locations (Figure 3M-P, Table 1), suggesting tumor propagation is governed primarily by cell-intrinsic factors rather than environment.

Unipotent CGNP are competent to produce medulloblastoma

In myeloid oncogenesis, multipotent cells rather than more restricted progenitor cells are thought to be the origin of leukemia stem cells (Faber and Armstrong, 2007). To test whether a restricted neuronal precursor can also give rise to MB, we activated SmoM2 in committed CGNP. *Math1-cre* drives expression within CGNP of the rRL and the entire EGL until P7-10, but not in PN, AS or IN (Machold and Fishell, 2005; Wang et al., 2005). In contrast, expression of the transcription factor *Tlx3 (Hox11L2)* is only seen in the EGL of Lobes VI-IX, but never in other lobes or the rRL (Suppl. Figure 2). Transgenic *Math1-cre* mice were generated using regulatory sequences 4 kb upstream of *Math1* (Matei et al., 2005; Schüller et al., 2007) and *Tlx3-cre* mice were generated by gene targeting of *Tlx3* (Xu et al., 2008). Fate mapping crosses involving a conditional *ROSA26-eYFP*$^{Fl/Fl}$ reporter confirmed that *Math1*$^+$ and *Tlx3*$^+$ precursors contributed solely to the GC lineage (Figure 4A-H and data not shown).

When crossed with *SmoM2*$^{Fl/Fl}$ mice, all *Math1*-cre animals developed MBs that could be transplanted into the cerebella of SCID mice (Figure 4I, J, Table 1, also see (Yang et al., 2008)). *Tlx3*-cre:*SmoM2* animals developed tumors in a posterior distribution in accord with the *Tlx3* expression domain (Figure 4K, L). These data show that unipotent CGNP are capable of tumor formation when targeted with oncogenic SmoM2. The Shh transcriptional target, Gli1, is expressed in proliferating CGNP (Wechsler-Reya and Scott, 1999) and we could induce MB formation in *Gli1-creERT2:SmoM2* mice until P14, but not at later postnatal stages.

Medulloblastomas exhibit a common phenotypic endpoint despite diverse cellular origins

To determine whether significant cellular (i.e. glial and neuronal diversity) and gene expression differences might exist in tumors derived from multipotent (e.g. *hGFAP-cre*) versus unipotent (e.g. *Math1-cre*) progenitor populations we performed Affymetrix gene expression profiling analyses, previously demonstrated to aid in distinguishing MB from other histologically similar primitive neuroectodermal tumors (Pomeroy et al., 2002). Comparison of expression profiles of the different murine tumors and *Ptc*$^{+/-}$ medulloblastoma using principal component (PC) analysis confirmed that all tumors had a gene expression signature of medulloblastomas and were highly related to each other (Figure 5A). Along the PC1 coordinate — the direction of greatest transcriptomic sample variance in cerebellar development —centroids of the MB tumor profiles were significantly different from matched normal samples ($p < 10^{-6}$). However, PC1 coordinate centroids were not significantly different for tumors derived from early (i.e., *hGFAP*- or *Olig2-cre*) versus late/unipotent (i.e., *Math1*- or *Tlx3-cre*) GC lineage progenitors (Suppl. Figure 3). In fact, only a very small number of genes (~150 of 54,675 probes tested) were found to be uniquely and differentially expressed in each tumor sub-group. In line with this, extensive histological (Figures 3C, 3G, 4J, 4L) and immunohistochemical analysis (Figure 5B) failed to reveal any clear differences in the cellular composition of the tumors. Furthermore, hierarchical cluster analysis based on the 150 genes differentially expressed amongst the tumors did not show strict clustering of tumors based on cell of origin (Suppl. Figure 4). Together, these findings indicate that tumors derived from early (i.e., *hGFAP-cre* or *Olig2-cre*) or late/unipotent (i.e., *Math1-cre* or *Tlx3-cre*) GC lineage progenitors arrive at a common phenotypic endpoint.

Cells expressing Gfap and Olig2 in Hh-activated medulloblastomas are neoplastic

All mouse tumors analyzed showed histological features in common with some human MBs including expression of CGNP markers (Math1, Zic, Pax6), Gfap, a marker usually found to be expressed in astrocytes, and Olig2, which is required for OL development (Lu et al., 2002) (Figure 5C). Clinical symptoms of tumor burden in *Math1-cre:SmoM2* tumors developed at an average age of 41 days (Table 1), however we found evidence of hyperplasia in the EGL at P0 and more clearly at P7 (Figure 6A, C). Strikingly, high expression of Olig2 was also found in these regions (Fig 6B, D). At P7, when the EGL is clearly discerned, excessive numbers of Olig2^{+} cells were observed in the EGL but not RL of *Math1-cre:SmoM2* mice (Figure 6D). Indeed, although Olig2^{+} cells that co-expressed Pax6 (Figure 1I) or a Math1 proxy marker (Figure 6E) could be observed at antenatal stages until E18, such co-labeled cells were not detectable at P7 (Figure 6F) or later stages. Thus, persistent Olig2 expression in the EGL of *Math1-cre:SmoM2* mice represents an early molecular marker of a pre-neoplastic state.

We found that only about 2% of mitotically active phosphoH3^{+} (pH3) cells were Olig2^{+} in fully developed *Math1-cre:SmoM2* tumors (Figure 6G). Indeed, the vast majority of proliferating cells were Cre^{+} (Figure 6H), a proxy for *Math1* expression, indicating that most cells contributing to MB growth are CGNP-like. In human tumors it is controversial whether cells expressing GFAP (or OLIG2) comprise tumor, or alternatively, represent intermingled cells from the normal brain. This is a critical point given that glial differentiation within MB would provide further evidence for a multipotent stem cell-like progenitor. To establish the

nature of cells comprising MB, we dissociated *Math1-cre:SmoM2* tumors and found that the SmoM2-YFP fusion protein, a marker of cells bearing the tumorigenic mutation, co-localized in cells expressing either Pax6, NeuN, Gfap or Olig2. Quantification revealed that YFP proteins co-localized with most if not all $Pax6^+$, $Olig2^+$ and $Gfap^+$ (100%, 90%, 96%, respectively) cells in acutely dissociated tumors (Figure 6I-L). In addition, we identified Olig2 and $Gfap^+$ cells that co-expressed the YFP reporter *in vivo* (Figure 6M, N). Thus, Olig2- and $Gfap^+$ cells are tumor cells rather than infiltrated/normal glial cells.

The $Gfap^+$ and $Olig2^+$ cells might represent simple astroglial and oligodendroglial tumor components. However, examination of $Gfap^+$ and $Olig2^+$ cells of the cerebellar anlagen (Figure 1) suggested that such tumor cells could, alternatively, retain features of primitive CGNP. In support of the latter possibility, we found that 81% of Olig2 cells expressed Pax6 and that 100% of $Gfap^+$ cells expressed Pax6 in acutely disassociated *Math1-cre:SmoM2* tumors *in vitro* (Figure 6O, P). These findings indicate that cells with an immature/progenitor phenotype are present in Hh-activated MB.

Human medulloblastoma contain rare OLIG2$^+$ cells with progenitor features

In order to determine the significance our findings might have for human MB, we examined $OLIG2^+$ cell populations within a cohort of human MBs. Although our original findings in mice were all in the setting of Shh/Smo pathway activation, we found that $OLIG2^+$ cells were present in both classic (40%) as well as desmoplastic (Shh-related) (77%) subtypes of human MBs (Fig 7A-D; Suppl. Table 1), and comprised less than 5% of cells in all tumors. Fluorescent in situ hybridization (FISH) analysis showed that $OLIG2^+$ cells in human MB contained copy number gain at the *C-MYC* locus, confirming them as tumor cells and arguing against the possibility that they might represent intermingled normal cells (Figure 7E, F). As further support for $OLIG2^+$ cells being tumor cells we identified co-expression of OLIG2 and the terminal neuronal differentiation marker, NEUN, in rare cells within human tumors (Figure 7G), and we found rare $OLIG2^+$ cells that expressed the proliferation marker, Ki67 (Figure 7H). Together, these data suggest the possibility that some $OLIG2^+$ cells are tumor cells with immature features and may represent a type of MB progenitor cell.

To mechanistically assess the lineage differentiation potential of $Olig2^+$ cells in the context of MB, we acutely disassociated tumors from *Olig2-tva-cre:SmoM2* mice and infected these cultures with RCAS-GFP viruses, to perform fate mapping of tumor stem/progenitor cells (Figure 7I). In our experimental paradigm, cells must be Olig2-tva^+ for infection with RCAS-GFP to occur. After six days in culture, we found that cells derived from $Olig2^+$ progenitors expressed Pax6, Zic or NeuN (Figure 7K-N). Significantly, of the 561 GFP^+ cells counted, only 68 (12%) expressed Olig2 on Day 6 (Figure 7J, N), indicating differentiation along GC lineage axis with down-regulation of Olig2. Upon acute harvest and disassociation of tumors (Day 0), we found that only 8% expressed Olig2. Of these, 66% co-expressed Pax6 and 12% expressed NeuN (Figure 7O-Q). Contrasting this, on Day 6 in the tva fate map experiment, 52% of Olig2-derived progeny expressed NeuN. These data are consistent with the proposal that $Olig2^+Pax6^+$ cells lose Olig2 expression and progress to express the more mature markers such as Zic and NeuN during the 6 days in culture. We conclude that $Olig2^+$ cells in *Olig2-tva-cre:SmoM2* tumors have the potential to produce GC-like progeny therefore supporting the possibility that they represent a subset of MB progenitor cells.

Discussion

Here we show that unipotent CGNP derive from multilineage embryonic CNS progenitors and that both populations are capable of generating MB when targeted with oncogenic SmoM2. Despite diverse origins, resulting tumors were similar leading to the conclusion that acquisition of CGNP identity is a critical determinant of progenitor cell competence to form Hedgehog-

induced MB. These findings provide insight into MB origins with implications for development of targeted cellular therapies.

Olig2+ progenitors of RL give rise to a subset of granule cell neurons

By creating a knock-in transgenic mouse line, *Olig2-tva-cre*, we targeted Olig2$^+$ cells using two fate map approaches. *Olig2-tva-cre* intercrossed with conditional reporters (e.g., *ROSA26-YFP*) mapped a subset of GC in the EGL and IGL of posterior CB. We then confirmed that these cells are derived from Olig2$^+$ progenitors in the rRL by *in utero* infection of *Olig2-tva-cre* mice with an avian RCAS retrovirus reporter. Although we cannot exclude that Olig2$^+$ cells outside of rRL could contribute to CGNP, this possibility seems unlikely given previous work that has established the rRL as the source of the GC lineage. These data indicate that rRL Olig2$^+$ progenitors give rise to a subset of GC (Figure 8A), which might contribute to functional heterogeneity (Zong et al., 2005).

Oncogenic signaling and lineage-restricted factors cooperate to determine tumor competence in CNS progenitors

Human inherited cancer syndromes show tumor formation in only a subset of cells within specific lineages despite germline transmission of tumor promoting mutations (e.g., *p53, pRB*-loss-of-function). Although several reports indicate that the Hh pathway is active in low- and high-grade gliomas (Ehtesham et al., 2007; Clement et al., 2007), in human Goltz-Gorlin syndrome, inherited heterozygous mutation of *PTCH* or *SUFU* lead to MB, but not gliomas. We failed to detect gliomas despite robust SmoM2 activation in forebrain progenitors, including developing neural stem cells and persistent progenitors of the SVZ and cortex expressing GFAP (Doetsch et al., 1999), NG2/Olig2 (Ligon et al., 2006) and Gli1 (Machold et al., 2003; Ahn and Joyner, 2005). Further work is needed to establish whether additional mutations (e.g., loss of *p53*) in concert with Hh activation might be necessary to enable glioma formation. Another possibility is that Shh activation biases towards neuronal lineage versus glial differentiation and therefore a MB phenotype and not glial lineages or glial tumor phenotype. Although we cannot rule this out, we think this explanation is unlikely for the following reasons. First, assuming that Shh promotes neuronal tumorigenesis, then one might expect to see development of such tumors at other CNS sites (e.g. supratentorial PNETs); this is not observed in human Goltz-Gorlin syndrome patients or in the mouse models we have studied. Second, we did not see other neuronal tumor types in the CB despite activation of Shh in PN and IN (Table 1). Third, we have recently shown that SmoM2 activation in the dentate gyrus causes hypertrophy but not cancer (Han et al., 2008).

Acquisition of granule cell lineage identity is critical for Hh-induced medulloblastoma formation

To identify progenitors competent for MB formation, we activated SmoM2 in a spectrum of stage- and position-specific progenitors during CGNP development. Both multipotent (e.g., *hGFAP*$^+$ and *Olig2*$^+$) progenitor populations within the cerebellar anlage as well as unipotent/restricted CGNP readily gave rise to MB with 100% penetrance. Despite these diverse origins, all SmoM2-activated MBs we analyzed exhibited a strikingly similar tumor phenotype at histological, immunohistochemical and expression profiling levels. The common final tumor phenotype is consistent with (1) a common cell or origin for all tumors, or (2) initial origins from *any* stem/progenitor which later converge on an amplifying CGNP-like tumor cell that dominates the ultimate phenotype (see Figure 8C). In either case, these findings support the conclusion that acquisition of CGNP identity is important for Hh-induced MB formation. Because orthotopically transplanted *Olig2-tva-cre:SmoM2* tumors were able to grow within the forebrain and CB, restriction of tumor susceptibility is evidently governed by cell-intrinsic

factors. Further work is needed to identify the underlying molecular determinants of CGNP "tumor competence" that lead to MB formation.

Hh-activated medulloblastoma can be generated in the EGL independent of VZ contributions

Human desmoplastic and classic MB have been suggested to arise from CGNP EGL (Schüller et al., 2005; Bühren et al., 2000) or progenitors of the VZ (Salsano et al., 2007; Katsetos et al., 1995), respectively. Our studies demonstrate that Hh-induced MB can be initiated by precise restriction of activating mutations to the EGL using *Tlx3-cre:SmoM2* and postnatally-induced *Gli1-creERT2:SmoM2* without activation of SmoM2 in the less differentiated cell populations of the rRL or VZ. Furthermore, while the time of tumor onset and the degree of tumor distribution varied depending on the cre drivers used (Table 1, Figure 8B), these variations appear to be based on the number/extent/ location of the total CGNP population targeted (i.e., broad diffuse versus small lateral populations). In addition, tumor masses never developed in the VZ or rRL proper, suggesting that further work will be needed to determine whether additional oncogenic pathways (e.g. MYC, Wnt) might lead to MB formation in these regions.

Evidence that Gfap+ and Olig2+ cells in medulloblastomas are neoplastic

Our data highlight that both mouse and human MBs exhibit extensive cellular heterogeneity. $GFAP^+$ cells are commonly identified in human MB (Schüller et al., 2004) and the morphology of those cells ranges from small tumor cells with a relatively large nucleus and a sparse, ring-like cytoplasm to cells with a rather differentiated phenotype and branched processes. We observed that $OLIG2^+$ cells, present in human MB, also varied in size and morphology. Using MYC FISH in human MB and YFP tracer expression in murine MB we demonstrate that $OLIG2^+$ and $GFAP^+$ cells are bona fide tumor cells and not just infiltrating cells arising from the normal surrounding brain. In addition we found small numbers of proliferating $Olig2^+$ and $Gfap^+$ cells within mouse and to a lesser degree human MB as further evidence that these heterogeneous elements represent tumor cells.

In human gliomas OLIG2 is expressed in tumor stem/progenitor cells and maintains the proliferation competence of both normal and tumorigenic progenitors of the murine forebrain (Ligon et al., 2007). However, given our data that OLIG2 is only rarely expressed in proliferating cells and is only present in 40% of classic and 77% of desmoplastic human MB cases, it seems clear that MB tumor growth is largely driven by rapidly dividing progenitor cells with CGNP characteristics, rather than $OLIG2^+$ cells. Might $GFAP^+$ and $OLIG2^+$ cells in MBs have other roles as relatively quiescent tumor progenitor cells? Our *in vitro* tumor fate mapping demonstrates that Hh-transformed $Olig2^+$ cells from murine MB can produce GC lineage-like progeny with advanced differentiation measured by NeuN labeling. Whether $Olig2^+$ tumor cells from other mouse models (i.e., non-Olig2-cre derived) have this capability remains to be determined.

Our data suggest that GFAP and OLIG2 expression in MB is not associated with "differentiated" astrocytes and oligodendrocytes. While almost all $Gfap^+$ and $Olig2^+$ cells in Hh-activated murine MB co-expressed Pax6 and other CGNP markers, the "biphenotypic" (e.g., OLIG2-NEUN) staining pattern is unlikely to be a specific consequence of Hh signaling, because we also observed this phenomenon in classic MBs, which are not associated with Hh mutations (Pietsch et al., 1997). We suggest that GFAP and OLIG2 label cells with a phenotype reminiscent of radial glia and less differentiated CGNP progenitors of the rRL (Figure 8A).

Does medulloblastoma arise from a multipotent stem cell?

MB was one of the first solid tumors for which "cancer stem cells" were reported (Hemmati et al., 2003). Cancer stem cells are classically described to be a tumor subpopulation with (1)

unlimited capacity for self-renewal and the ability to regenerate tumor upon transplantation, and (2) the potential to produce multilineage progeny similar to distinct cell types of a cognate organ (Reya et al., 2001). The question of authentic glial cell production has critical implications for understanding MB progenitors and their characterization as multipotent cancer stem cells. However, evidence for multilineage differentiation of MB stem cells has been based on the expression of relatively few neuronal and glial cell markers with uncertain relation to either differentiated cell types of the CB or CNS multipotent stem cells. For example, the commonly used marker, GFAP, marks Type B stem cells of the subventricular zone (Doetsch et al., 1999). We show that Gfap and Olig2 mark cells in MBs reminiscent of those found during early CGNP development, but not differentiated glia. These findings argue against existence of MB progenitors with multilineage (neuronal and glial) contributions to the tumor mass. However, they are consistent with the possibility that MB could originate from either a multipotent or unipotent progenitor (Figure 8C).

We used lineage tracing to clarify the possible relationship between cells found during GC lineage development and those that are tumor-competent to produce MB. Our findings highlight distinctions between "cell-of-origin" (that acquires the oncogenic mutation) and "tumor-propagating" cell, responsible for major growth and phenotypic characteristics of the ultimate tumor. For instance, if unipotent cell identity ("Type C2") is necessary for tumor growth (Figure 8C), then a tumor arising from mutation of a Type A or Type C2 cell would appear identical notwithstanding their different cells-of-origin. This also raises the possibility of a "de-differentiation" pathway to produce tumors with mixed multipotent and unipotent features, as has been suggested for certain leukemia stem cells (Krivtsov et al., 2006). Although our data do not provide direct evidence for de-differentiation, tumors from postnatally-induced *Gli1-creERT2:SmoM2* (J. Mao, A. McMahon and K. Ligon, unpublished observations) and *Math1-creERT2:Ptc*$^{Fl/Fl}$ animals (Z. J. Yang and R. J. Wechsler-Reya, unpublished observations) contain many Olig2^{+} cells, consistent with the possibility that late-stage CGNP can adopt less-differentiated characteristics (Figure 8). Further investigation is needed to determine whether dedifferentiation of mature granule cells (D2 >C2) constitutes a biologically feasible or clinically relevant pathway of tumor formation.

Experimental Procedures

Animal Procedures

For fate mapping, various *cre*-strains (Table 1) were intercrossed with *ROSA26-eYFP*$^{Fl/Fl}$ or *CAG-CAT-eGFP*$^{Fl/Fl}$ conditional reporter mice. At least three cerebella were harvested for each different time point fixed overnight in 4% paraformaldehyde/PBS. For tumor generation, *cre*-strains were intercrossed with *SmoM2*$^{Fl/Fl}$ mice and followed for survival and subsequent Kaplan-Meier analysis. For injections into forebrains or cerebella of SCID mice, tumor cells were freshly dissociated and resuspended in 1 μl PBS at a concentration of 10^5/μl (see Suppl. Methods). See Supplemental Methods for detailed information on generation, acquisition and genotyping of transgenic mouse strains and procedures including RCAS infection of *Olig2-tva-cre* embryonic hindbrain. All animal procedures were approved by the Institutional Animal Care and Use Committees at DFCI and UCSF.

Tissue collection, histological analysis, immunohistochemistry (IHC), in situ hybidization and photomicroscopy

Human tissue samples were obtained in accordance with the rules and regulations for human tissue collection; use in this study was approved by the Institutional Review Boards of the Brigham and Women's Hospital/Partners Healthcare and Children's Hospital Boston. Tissue samples were processed using standard techniques. Detailed protocols for in situ hybridization and immunohistochemistry, immuno-FISH as well as all antibodies used in this study are listed

in Supplemental Methods and are available on request. Photomicrographs were taken with Zeiss Axioskop/Axiocam imaging or Nikon E600/SPOT imaging systems. For whole mount pictures of mouse MBs, fluorescent and bright-field images were overlaid using Photoshop software. A Leica TCS SL system was used for confocal microscopy.

Cell culture

Cultures from *Math1-cre:SmoM2* tumors were established by triturating tumor tissue in DMEM medium and plating the cells on poly-D-Lysine coated dishes. Acutely dissociated *Math1-cre, SmoM2* tumor cells were fixed 12 hours after plating. Long-term cultures were analyzed after 4 weeks in culture and 3 passages. Immunostaining was performed as described above. Cells from *Olig2-tva-cre:SmoM2* tumors were infected with virus carrying *RCAS(A)-GFP* (2×10^7 cfu/ml; gift of C. Cepko, Harvard Medical School) after 24 hr culture in serum-free medium. Serum-containing medium was then added; after a total culture time of 6 days, cells were fixed and stained.

Statistics and quantification

For *in vivo* fate mapping in *Olig2-tva-cre* mice, counts were derived from analysis of 3 independent animals, and at least 10 20X fields of labeled sections of CB focused around Lobe X. For cell culture counts, cells were derived from pups of at least four separate litters. Each litter yielded material for two six-well plates of cerebellar and one six-well plate of ventricular cultures. Three wells of a six-well plate were used for each treatment (EGF, Shh, vehicle). At least 100 cells were assessed in each sample to determine the fraction of $Olig2^+$, Zic^+ or $Gfap^+$ cells. Statistical analysis was performed using the unpaired Student's *t*-test with a two-tailed *p*-value.

Microarray Data and Analysis

The transcriptome of 21 cre-activated tumors and control cerebellar tissues were profiled using the Affymetrix GeneChip Mouse Genome 430 2.0 Plus [http://www.ncbi.nlm.nih.gov/geo/query/acc.cgi?acc=GSE11859]. Transcriptomes of the developing mouse CB P1-60 were profiled using the Affymetrix Murine Mu11K set as described previously (Kho et al., 2004) and principal component analysis (PCA) was used to determine the global similarity and variation between the transcriptome profiles of the different tissues (Johnson and Wichern, 2002). For detailed description, see supplementary methods.

Supplementary Material

Refer to Web version on PubMed Central for supplementary material.

Acknowledgements

The authors are grateful to Rob Wechsler-Reya for sharing unpublished data, to Charles D. Stiles for comments and to Jason Ling, Sovann Kaing, Dong-in Yuk, Natalie Vena and Emily Learner for expert technical assistance. U.S. was supported by a fellowship from the Dr. Mildred-Scheel-Stiftung für Krebsforschung and by the Max-Eder-Nachwuchsgruppenprogramm of the Deutsche Krebshilfe. V.M.H. thanks the Netherlands Organization for Scientific Research (NWO) for a TALENT-stipend. J.M. was supported by a grant from the Charles King Trust Medical Foundation. Y-G. H., A.K.D. and E.H. thank the American Brain Tumor Foundation for support. This work was supported by grants from the NIH to K.L.L. (NS047213), A.K. (NS040828). A.P.M. (NS033642) and D.H.R. (NS047527), the James S. McDonnell Research Foundation (to D.H.R.), the March of Dimes Foundation (to D.H.R.), and a grant from the Pediatric Brain Tumor Foundation of the United States (to A.A-B. and D.H.R.). D.H.R is a HHMI Investigator. All authors declare that they have no competing financial interests.

References

Abraham H, Tornoczky T, Kosztolanyi G, Seress L. Cell formation in the cortical layers of the developing human cerebellum. Int. J. Dev. Neurosci 2001;19:53–62. [PubMed: 11226755]

Ahn S, Joyner AL. In vivo analysis of quiescent adult neural stem cells responding to Sonic hedgehog. Nature 2005;437:894–897. [PubMed: 16208373]

Altmann, J.; Bayer, SA. Development of the Cerebellar System in Relation to its Evolution, Structure and Functions. CRC Press; New York: 1997.

Barabe F, Kennedy JA, Hope KJ, Dick JE. Modeling the initiation and progression of human acute leukemia in mice. Science 2007;316:600–604. [PubMed: 17463288]

Ben Arie N, Bellen HJ, Armstrong DL, McCall AE, Gordadze PR, Guo Q, Matzuk MM, Zoghbi HY. Math1 is essential for genesis of cerebellar granule neurons. Nature 1997;390:169–172. [PubMed: 9367153]

Borghesani PR, Peyrin JM, Klein R, Rubin J, Carter AR, Schwartz PM, Luster A, Corfas G, Segal RA. BDNF stimulates migration of cerebellar granule cells. Development 2002;129:1435–1442. [PubMed: 11880352]

Bühren J, Christoph AH, Buslei R, Albrecht S, Wiestler OD, Pietsch T. Expression of the neurotrophin receptor p75NTR in medulloblastomas is correlated with distinct histological and clinical features: evidence for a medulloblastoma subtype derived from the external granule cell layer. J. Neuropathol. Exp. Neurol 2000;59:229–240. [PubMed: 10744061]

Casper KB, McCarthy KD. GFAP-positive progenitor cells produce neurons and oligodendrocytes throughout the CNS. Mol. Cell Neurosci 2006;31:676–684. [PubMed: 16458536]

Clement V, Sanchez P, de Tribolet N, Radovanovic I, Altaba A. HEDGEHOG-GLI1 signaling regulates human glioma growth, cancer stem cell self-renewal, and tumorigenicity. Curr. Biol 2007;17:165–172. [PubMed: 17196391]

Cobaleda C, Jochum W, Busslinger M. Conversion of mature B cells into T cells by dedifferentiation to uncommitted progenitors. Nature 2007;449:473–477. [PubMed: 17851532]

Dahmane N, Altaba A. Sonic hedgehog regulates the growth and patterning of the cerebellum. Development 1999;126:3089–3100. [PubMed: 10375501]

Doetsch F, Caille I, Lim DA, Garcia-Verdugo JM, Alvarez-Buylla A. Subventricular zone astrocytes are neural stem cells in the adult mammalian brain. Cell 1999;97:703–716. [PubMed: 10380923]

Ehtesham M, Sarangi A, Valadez JG, Chanthaphaychith S, Becher MW, Abel TW, Thompson RC, Cooper MK. Ligand-dependent activation of the hedgehog pathway in glioma progenitor cells. Oncogene 2007;26:5752–5761. [PubMed: 17353902]

Engelkamp D, Rashbass P, Seawright A, van H,V. Role of Pax6 in development of the cerebellar system. Development 1999;126:3585–3596. [PubMed: 10409504]

Faber J, Armstrong SA. Mixed lineage leukemia translocations and a leukemia stem cell program. Cancer Res 2007;67:8425–8428. [PubMed: 17875678]

Fuccillo M, Joyner AL, Fishell G. Morphogen to mitogen: the multiple roles of hedgehog signalling in vertebrate neural development. Nat. Rev. Neurosci 2006;7:772–783. [PubMed: 16988653]

Galli R, Binda E, Orfanelli U, Cipelletti B, Gritti A, De Vitis S, Fiocco R, Foroni C, DiMeco F, Vescovi A. Isolation and characterization of tumorigenic, stem-like neural precursors from human glioblastoma. Cancer Res 2004;64:7011–7021. [PubMed: 15466194]

Hahn H, Wojnowski L, Miller G, Zimmer A. The patched signaling pathway in tumorigenesis and development: lessons from animal models. J. Mol. Med 1999;77:459–468. [PubMed: 10475061]

Han YG, Spassky N, Romaguera-Ros M, Garcia-Verdugo JM, Aguilar A, Schneider-Maunoury S, Alvarez-Buylla A. Hedgehog signaling and primary cilia are required for the formation of adult neural stem cells. Nat. Neurosci 2008;11:277–284. [PubMed: 18297065]

Hemmati HD, Nakano I, Lazareff JA, Masterman-Smith M, Geschwind DH, Bronner-Fraser M, Kornblum HI. Cancerous stem cells can arise from pediatric brain tumors. Proc. Natl. Acad. Sci. U.S.A 2003;100:15178–15183. [PubMed: 14645703]

Herms J, Neidt I, Lüscher B, Sommer A, Schurmann P, Schröder T, Bergmann M, Wilken B, Probst-Cousin S, Hernaiz-Driever P, Behnke J, Hanefeld F, Pietsch T, Kretzschmar HA. C-MYC expression in medulloblastoma and its prognostic value. Int. J. Cancer 2000;89:395–402. [PubMed: 11008200]

Johnson, RA.; Wichern, DW. Applied Multivariate Statistical Analysis. Upper Saddle River; Prentice Hall: 2002.

Johnson RL, Rothman AL, Xie J, Goodrich LV, Bare JW, Bonifas JM, Quinn AG, Myers RM, Cox DR, Epstein EH Jr. Scott MP. Human homolog of patched, a candidate gene for the basal cell nevus syndrome. Science 1996;272:1668–1671. [PubMed: 8658145]

Katsetos CD, Herman MM, Krishna L, Vender JR, Vinores SA, Agamanolis DP, Schiffer D, Burger PC, Urich H. Calbindin-D28k in subsets of medulloblastomas and in the human medulloblastoma cell line D283 Med. Arch. Pathol. Lab Med 1995;119:734–743. [PubMed: 7646332]

Kawauchi D, Taniguchi H, Watanabe H, Saito T, Murakami F. Direct visualization of nucleogenesis by precerebellar neurons: involvement of ventricle-directed, radial fibre-associated migration. Development 2006;133:1113–1123. [PubMed: 16501169]

Kho AT, Zhao Q, Cai Z, Butte AJ, Kim JY, Pomeroy SL, Rowitch DH, Kohane IS. Conserved mechanisms across development and tumorigenesis revealed by a mouse development perspective of human cancers. Genes Dev 2004;18:629–640. [PubMed: 15075291]

Krivtsov AV, Twomey D, Feng Z, Stubbs MC, Wang Y, Faber J, Levine JE, Wang J, Hahn WC, Gilliland DG, Golub TR, Armstrong SA. Transformation from committed progenitor to leukaemia stem cell initiated by MLLAF9. Nature 2006;442:818–822. [PubMed: 16862118]

Lee A, Kessler JD, Read TA, Kaiser C, Corbeil D, Huttner WB, Johnson JE, Wechsler-Reya RJ. Isolation of neural stem cells from the postnatal cerebellum. Nat. Neurosci 2005;8:723–729. [PubMed: 15908947]

Lee Y, Miller HL, Jensen P, Hernan R, Connelly M, Wetmore C, Zindy F, Roussel MF, Curran T, Gilbertson RJ, McKinnon PJ. A Molecular Fingerprint for Medulloblastoma. Cancer Res 2003;63:5428–5437. [PubMed: 14500378]

Lewis PM, Gritli-Linde A, Smeyne R, Kottmann A, McMahon AP. Sonic hedgehog signaling is required for expansion of granule neuron precursors and patterning of the mouse cerebellum. Dev. Biol 2004;270:393–410. [PubMed: 15183722]

Ligon KL, Huillard E, Mehta S, Kesari S, Liu H, Alberta JA, Bachoo RM, Kane M, Louis DN, Depinho RA, Anderson DJ, Stiles CD, Rowitch DH. Olig2-regulated lineage-restricted pathway controls replication competence in neural stem cells and malignant glioma. Neuron 2007;53:503–517. [PubMed: 17296553]

Ligon KL, Kesari S, Kitada M, Sun T, Arnett HA, Alberta JA, Anderson DJ, Stiles CD, Rowitch DH. Development of NG2 neural progenitor cells requires Olig gene function. Proc. Natl. Acad. Sci. U.S.A 2006;103:7853–7858. [PubMed: 16682644]

Lu QR, Sun T, Zhu Z, Ma N, Garcia M, Stiles CD, Rowitch DH. Common developmental requirement for Olig function indicates a motor neuron/oligodendrocyte connection. Cell 2002;109:75–86. [PubMed: 11955448]

Machold R, Fishell G. Math1 is expressed in temporally discrete pools of cerebellar rhombic-lip neural progenitors. Neuron 2005;48:17–24. [PubMed: 16202705]

Machold R, Hayashi S, Rutlin M, Muzumdar MD, Nery S, Corbin JG, Gritli-Linde A, Dellovade T, Porter JA, Rubin LL, Dudek H, McMahon AP, Fishell G. Sonic hedgehog is required for progenitor cell maintenance in telencephalic stem cell niches. Neuron 2003;39:937–950. [PubMed: 12971894]

Malatesta P, Hack MA, Hartfuss E, Kettenmann H, Klinkert W, Kirchhoff F, Götz M. Neuronal or glial progeny: regional differences in radial glia fate. Neuron 2003;37:751–764. [PubMed: 12628166]

Mao J, Ligon KL, Rakhlin EY, Thayer SP, Bronson RT, Rowitch D, McMahon AP. A novel somatic mouse model to survey tumorigenic potential applied to the Hedgehog pathway. Cancer Res 2006;66:10171–10178. [PubMed: 17047082]

Matei V, Pauley S, Kaing S, Rowitch D, Beisel KW, Morris K, Feng F, Jones K, Lee J, Fritzsch B. Smaller inner ear sensory epithelia in Neurog 1 null mice are related to earlier hair cell cycle exit. Dev. Dyn 2005;234:633–650. [PubMed: 16145671]

Morales D, Hatten ME. Molecular markers of neuronal progenitors in the embryonic cerebellar anlage. J. Neurosci 2006;26:12226–12236. [PubMed: 17122047]

Petryniak MA, Potter GB, Rowitch DH, Rubenstein JL. Dlx1 and Dlx2 control neuronal versus oligodendroglial cell fate acquisition in the developing forebrain. Neuron 2007;55:417–433. [PubMed: 17678855]

Pietsch T, Waha A, Koch A, Kraus J, Albrecht S, Tonn J, Sörensen N, Berthold F, Henk B, Schmandt N, Wolf HK, von Deimling A, Wainwright B, Chenevix-Trench G, Wiestler OD, Wicking C. Medulloblastomas of the desmoplastic variant carry mutations of the human homologue of Drosophila patched. Cancer Res 1997;57:2085–2088. [PubMed: 9187099]

Pomeroy SL, Tamayo P, Gaasenbeek M, Sturla LM, Angelo M, McLaughlin ME, Kim JY, Goumnerova LC, Black PM, Lau C, Allen JC, Zagzag D, Olson JM, Curran T, Wetmore C, Biegel JA, Poggio T, Mukherjee S, Rifkin R, Califano A, Stolovitzky G, Louis DN, Mesirov JP, Lander ES, Golub TR. Prediction of central nervous system embryonal tumour outcome based on gene expression. Nature 2002;415:436–442. [PubMed: 11807556]

Reya T, Morrison SJ, Clarke MF, Weissman IL. Stem cells, cancer, and cancer stem cells. Nature 2001;414:105–111. [PubMed: 11689955]

Rowitch DH, Jacques B, Lee SM, Flax JD, Snyder EY, McMahon AP. Sonic hedgehog regulates proliferation and inhibits differentiation of CNS precursor cells. J. Neurosci 1999;19:8954–8965. [PubMed: 10516314]

Salsano E, Croci L, Maderna E, Lupo L, Pollo B, Giordana MT, Consalez GG, Finocchiaro G. Expression of the neurogenic basic helix-loop-helix transcription factor NEUROG1 identifies a subgroup of medulloblastomas not expressing ATOH1. Neuro. Oncol 2007;9:298–307. [PubMed: 17522332]

Schüller U, Koch A, Hartmann W, Garre ML, Goodyer CG, Cama A, Sörensen N, Wiestler OD, Pietsch T. Subtype-specific expression and genetic alterations of the chemokinereceptor gene CXCR4 in medulloblastomas. Int. J. Cancer 2005;117:82–89. [PubMed: 15880586]

Schüller U, Schober F, Kretzschmar HA, Herms J. Bcl-2 expression inversely correlates with tumour cell differentiation in medulloblastoma. Neuropathol. Appl. Neurobiol 2004;30:513–521. [PubMed: 15488027]

Shih AH, Holland EC. Developmental neurobiology and the origin of brain tumors. J. Neurooncol 2004;70:125–136. [PubMed: 15674474]

Singh SK, Hawkins C, Clarke ID, Squire JA, Bayani J, Hide T, Henkelman RM, Cusimano MD, Dirks PB. Identification of human brain tumour initiating cells. Nature 2004;432:396–401. [PubMed: 15549107]

Spassky N, Han YG, Aguilar A, Strehl L, Besse L, Laclef C, Romaguera RM, Garcia-Verdugo JM, Alvarez-Buylla A. Primary cilia are required for cerebellar development and Shh-dependent expansion of progenitor pool. Dev. Biol 2008;317:246–259. [PubMed: 18353302]

Srinivas S, Watanabe T, Lin CS, William CM, Tanabe Y, Jessell TM, Costantini F. Cre reporter strains produced by targeted insertion of EYFP and ECFP into the ROSA26 locus. BMC. Dev. Biol 2001;1:4. [PubMed: 11299042]

Wang VY, Rose MF, Zoghbi HY. Math1 expression redefines the rhombic lip derivatives and reveals novel lineages within the brainstem and cerebellum. Neuron 2005;48:31–43. [PubMed: 16202707]

Warner JK, Wang JC, Hope KJ, Jin L, Dick JE. Concepts of human leukemic development. Oncogene 2004;23:7164–7177. [PubMed: 15378077]

Wechsler-Reya RJ, Scott MP. Control of neuronal precursor proliferation in the cerebellum by Sonic Hedgehog. Neuron 1999;22:103–114. [PubMed: 10027293]

Xu Y, Lopes C, Qian Y, Cheng L, Goulding M, Turner E, Lima D, Ma Q. Tlx1 and Tlx3 coordinate specification of dorsal horn pain-modulary peptidergic neurons. J. Neuroscience 2008;28:4037–4046.

Yamasaki T, Kawaji K, Ono K, Bito H, Hirano T, Osumi N, Kengaku M. Pax6 regulates granule cell polarization during parallel fiber formation in the developing cerebellum. Development 2001;128:3133–3144. [PubMed: 11688562]

Yang ZJ, Ellis T, Markant SL, Read TA, Kessler JD, Bourboulas M, Schüller U, Machold R, Fishell G, Rowitch DH, Wainwright B, Wechsler-Reya RJ. Medulloblastoma can be initiated in lineage-restricted progenitors or stem cells. Cancer Cell. 2008 In press.

Zhou Q, Anderson DJ. The bHLH transcription factors OLIG2 and OLIG1 couple neuronal and glial subtype specification. Cell 2002;109:61–73. [PubMed: 11955447]

Zong H, Espinosa JS, Su HH, Muzumdar MD, Luo L. Mosaic analysis with double markers in mice. Cell 2005;121:479–492. [PubMed: 15882628]

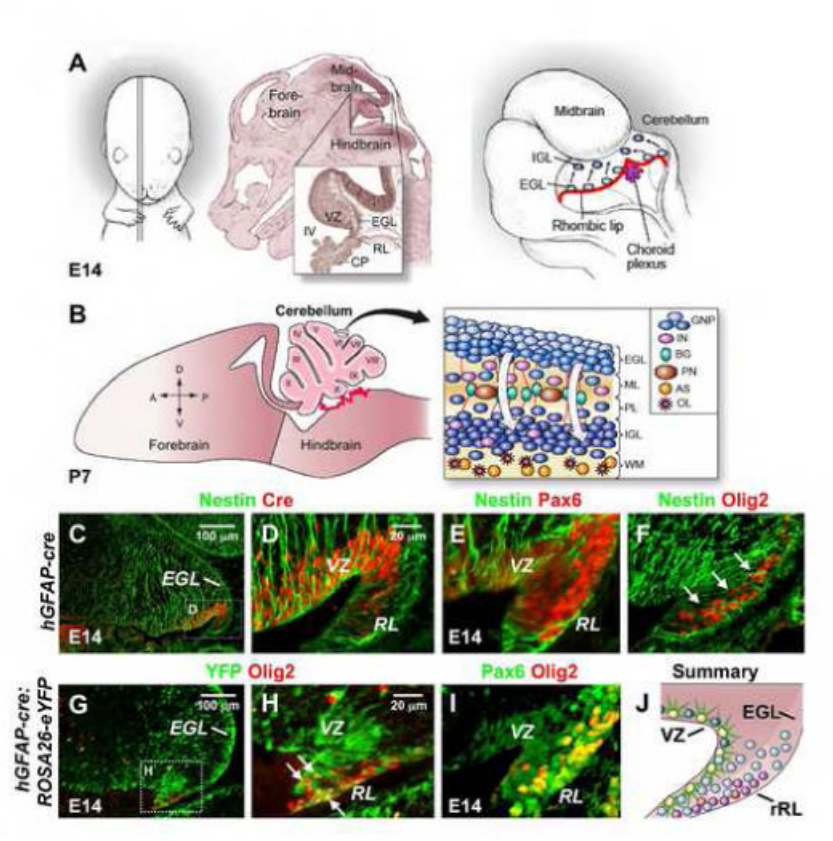

Figure 1. Identification of an Olig2^{+} progenitor population in the rostral RL

(A) The cerebellar anlagen at E14. The VZ and RL serve as mitotic niches at this age. The EGL is formed by proliferating CGNP that have left the RL. (B) At P7, the developing CB is divided into 10 lobes with defined cortical layers. (C-E) Sagittal sections at E14 in *hGFAP-cre* mice showing co-localization of Nestin, cre and Pax6 proteins in progenitor cells of the VZ and rRL. (F) Olig2 expression is largely restricted to dorsal rRL. (G, H) Fate mapping experiments (*hGFAP-cre* × *ROSA26-eYFP*$^{Fl/Fl}$ mice) reveals YFP in the EGL and a subset of RL cells that express Olig2 (arrows). (I) Olig2^{+} RL precursors co-label with the CGNP marker Pax6; some single Pax6^{+} precursors in the VZ were observed (arrows). (J) Summary of cells in the RL region at E14 showing relative positions of radial glia (yellow/green), Pax6 (blue) $^{+}$, Olig2(red)$^{+}$ and Pax6^{+}Olig2(purple)$^{+}$ cells. *BG*, Bergmann glia; *CP*, choroid plexus; *GNP*, granule neuron precursors; *ML*, molecular layer; *PL*, Purkinje cell layer.

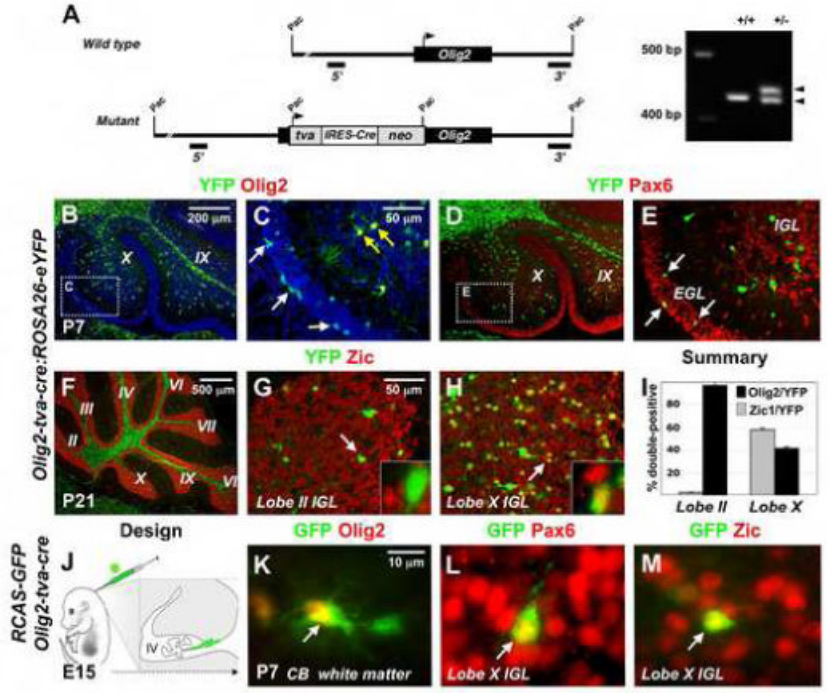

Figure 2. A subset of cerebellar granule neurons derive from Olig2$^+$ progenitors

(A)*Olig2-tva-cre* allele and genotyping of the respective mutant mice using PCR to generate wild type 429bp and mutant (cre) 446bp products. (B-I) Fate mapping of Olig2-expressing cells with *ROSA26-eYFP*$^{Fl/Fl}$ reporter. Co-localization of YFP and Olig2 proteins in sagittal sections of P7 cerebella reveals that YFP is expressed in oligodendrocytes within the cerebellar WM (yellow arrows in C) as well as in occasional cells within the EGL (white arrows). YFP-Pax6 labeling confirms the granule lineage character of YFP-expressing EGL cells (D, E, arrows). The IGL of P21 cerebella demonstrates lobe-specific differences in Olig2 fate mapping. (G) The IGL of Lobe II contains YFP$^+$ cells that predominantly co-express Olig2 (arrow and cell shown, inset) but not the GC marker Zic. In contrast, the IGL of Lobe X (H) contains numerous YFP/Zic double-positive cells (arrow and inset). (I) Mean percentage (+/- SEM) of Olig2$^+$YFP$^+$ and Zic1$^+$YFP$^+$ double-positive cells in the IGL of lobe II and X. (J-M) *In utero* fate mapping of Olig2-expressing cells by RCAS-GFP virus injection into the rRL of E15.5 *Olig2-tva-cre* mice. Analysis of the CB at P7 reveals GFP to be expressed in Olig2$^+$ (K) WM cells, as well as Pax6$^+$ (L) and Zic$^+$ (M) cells of the IGL in Lobe X.

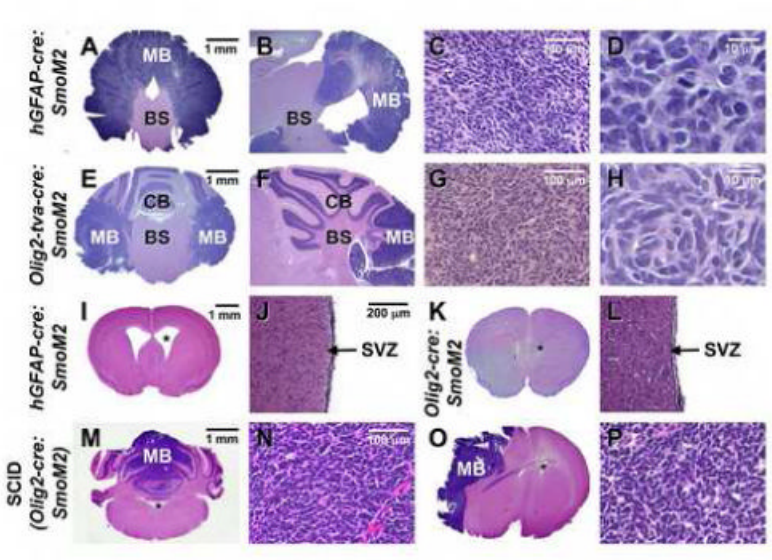

Figure 3. Development of medulloblastoma but not glioma from hGFAP$^+$ and Olig2$^+$ precursors

Targeting *hGFAP*$^+$ and *Olig2*$^+$ precursor cells with SmoM2 results in MB (A-H). While neoplastic transformation of *hGFAP*$^+$ cells affects the entire cerebellar cortex (A-D), MBs from *Olig2*-expressing precursors are restricted to posterior cerebellar regions (E-H). Although *hGFAP*-cre and *Olig2*-cre are broadly expressed in all parts of the CNS, neoplastic lesions due to SmoM2 are restricted to the CB. Forebrain sections including the subventricular zone (SVZ) in adult animals appear normal (I-L). Transplantation of *Olig2-tva-cre:SmoM2* tumor cells into SCID mice gives rise tumors both in hindbrain (M,N) and forebrain (O,P) regions. A, E and I-P are frontal, B-D and F-H are sagittal sections stained with H&E. C and D are high power magnifications from B, so are G and H from F. Asterisks mark lateral ventricles in I, K and O and the IVth ventricle in M. *BS*, brainstem.

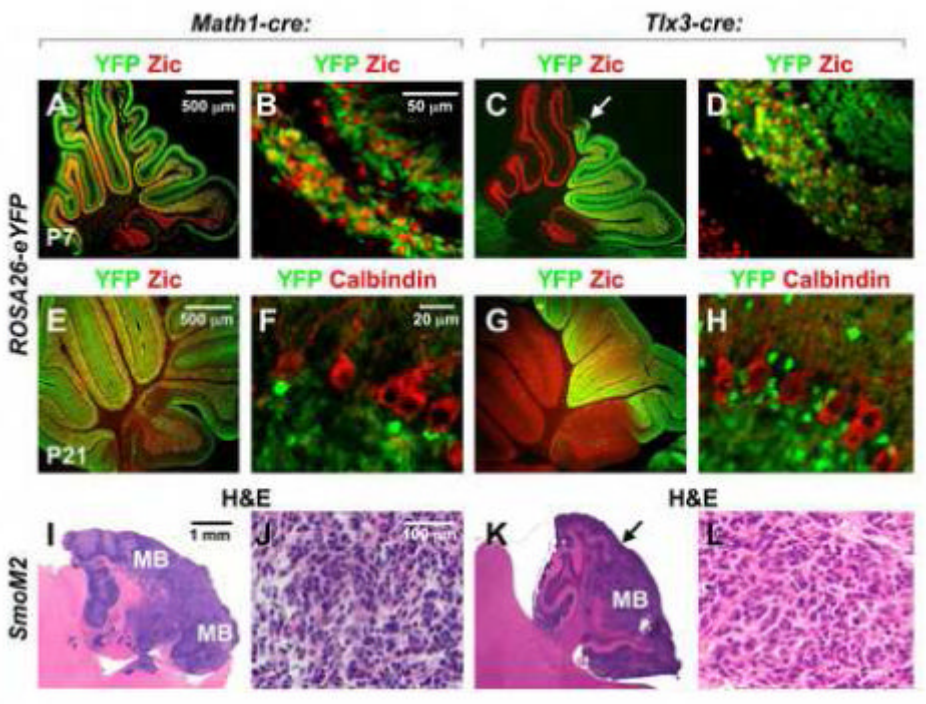

Figure 4. Late stage unipotent CGNP are competent to produce medulloblastoma

(A-H) Cre expression driven by *Math1* or *Tlx3* promoter sequences is normally restricted to granule lineage cell as shown by crosses with *Rosa26-eYFP* conditional reporter mice. (C, D, G) GC fate-mapped by *Tlx3*-cre are restricted to Lobes VI-IX. (F, H) In contrast, Calbindin-expressing PN do not derive from *Math1*$^{+}$ or *Tlx3*$^{+}$ precursors. (I-L) Both *Math1*$^{+}$ and *Tlx3*$^{+}$ granule neurons give rise to MB after activation of SmoM2, and *Tlx3-cre* driven tumors obeyed posterior restriction consistent with fate mapping (compare arrows in C, K).

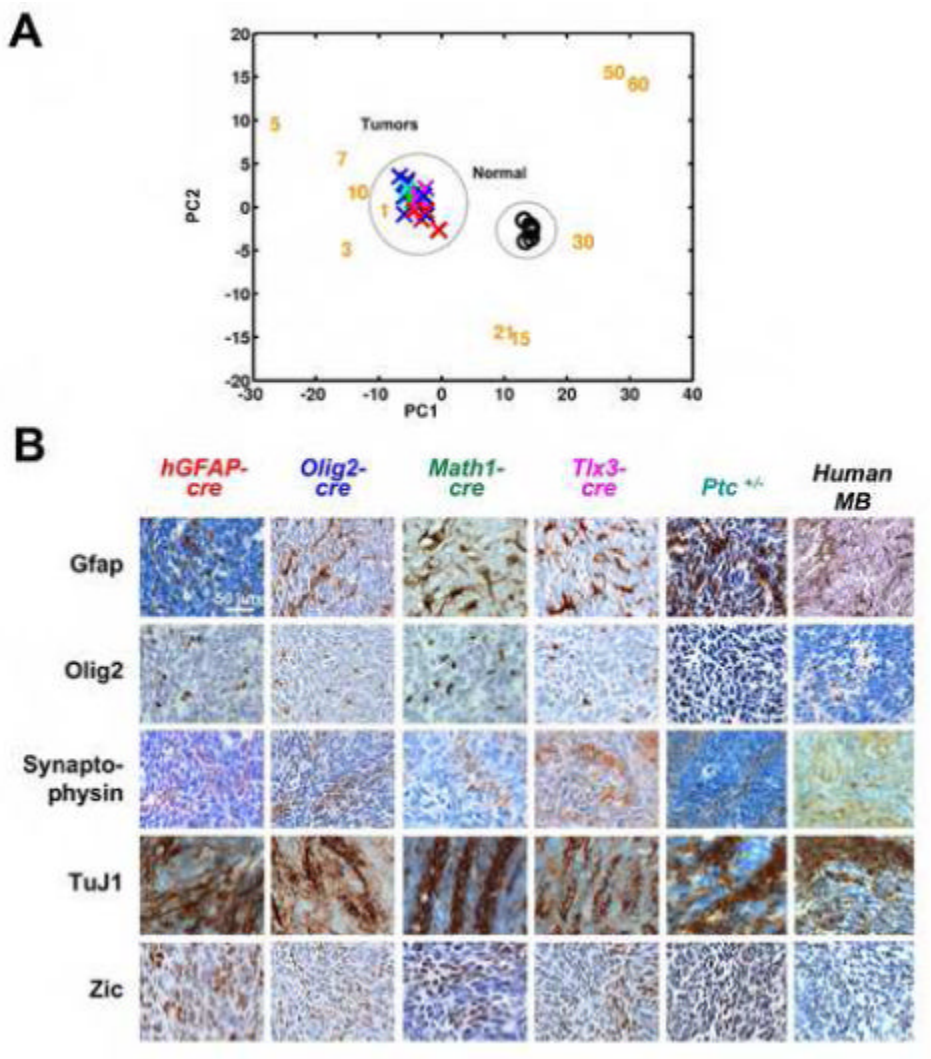

Figure 5. Medulloblastoma generated from diverse progenitor cell origins leads to a convergent phenotypic endpoint

(A) Principal component analysis of global gene expression in conditional MB models [*Math1* (green)-, *Tlx3*(magenta)-, *hGFAP*(red)-, *Olig2*(blue)-*cre:SmoM2* and *Ptc*$^{+/-}$ (turquoise)] and samples from normal littermate control CB (black circles) are mapped onto normal cerebellar developmental space as defined by a 7000 member, rank-normalized gene set (Kho et al., 2004), from developing CB at stages P1, 3, 5, 7, 10, 15, 21, 30, 50 and 60 (orange numbers). Tumors were related to early rather than late developmental stages of the CB as we have reported for human MB (Kho et al., 2004). (B) Immunohistochemical analysis confirms all murine tumors exhibit a similar immunohistochemical staining pattern to each other as well as human MB with respect to standard neuronal and glial neuropathological markers. Results are representative of at least two tumor samples.

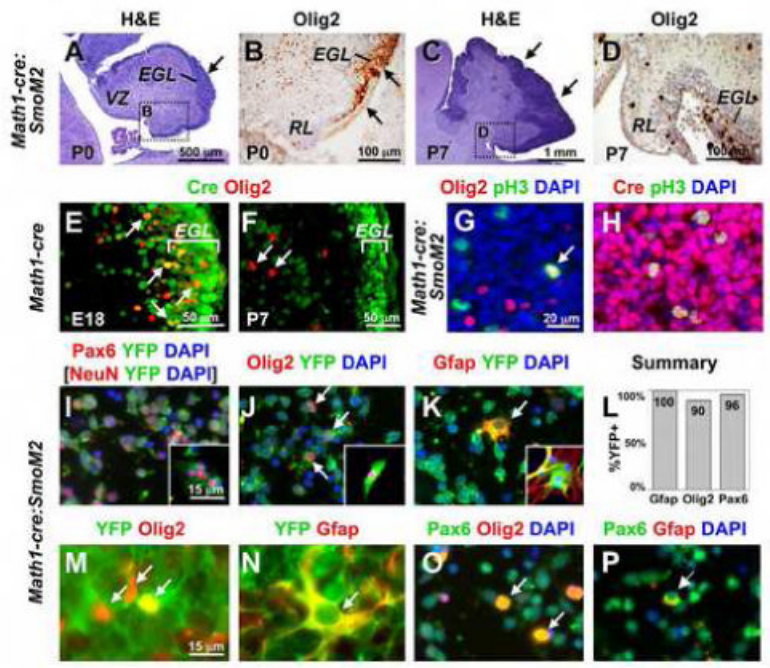

Figure 6. Olig2- and Gfap-expressing cells in medulloblastoma are neoplastic and have features in common with immature granule lineage precursors

(A, C) In *Math1-cre:SmoM2* animals, morphologic evidence hyperplasia is predominantly observed in the EGL, but not RL or VZ, at P0 and is more apparent by P7. (B, D) Greatly increased numbers of Olig2$^+$ cells were observed in hyperplastic regions of the EGL--but not RL--of P0 and P7 *Math1-cre:SmoM2* mice. (E, F) Expression of cre proteins in *Math1-cre* mice co-localized with Olig2 at E18 but not P7. (G) Olig2 co-expression was detected in only ~2% of pH3$^+$ cells in tumors. (H) In contrast, ~98% of pH3$^+$ cells co-labeled with cre proteins. (I-K) Phenotype of acutely disassociated cells and (insets) cells cultured from MB for four weeks. While most of dissociated *Math1-cre:SmoM2* tumor cells express the GC markers Pax6 or (inset) NeuN (I), some express Olig2 (J) and Gfap (K). SmoM2 is fused to YFP, which therefore marks tumor cells. (L) Cell counting reveals that more than 90% of cells expressing Gfap, Olig2 and Pax6 are tumor cells, as shown by co-expression of YFP. (M, N) Immunohistochemistry of tumor sections demonstrates similar results. (O) 81% of Olig2$^+$ and (P) 100% of Gfap$^+$ cells in tumors expressed the CGNP marker Pax6.

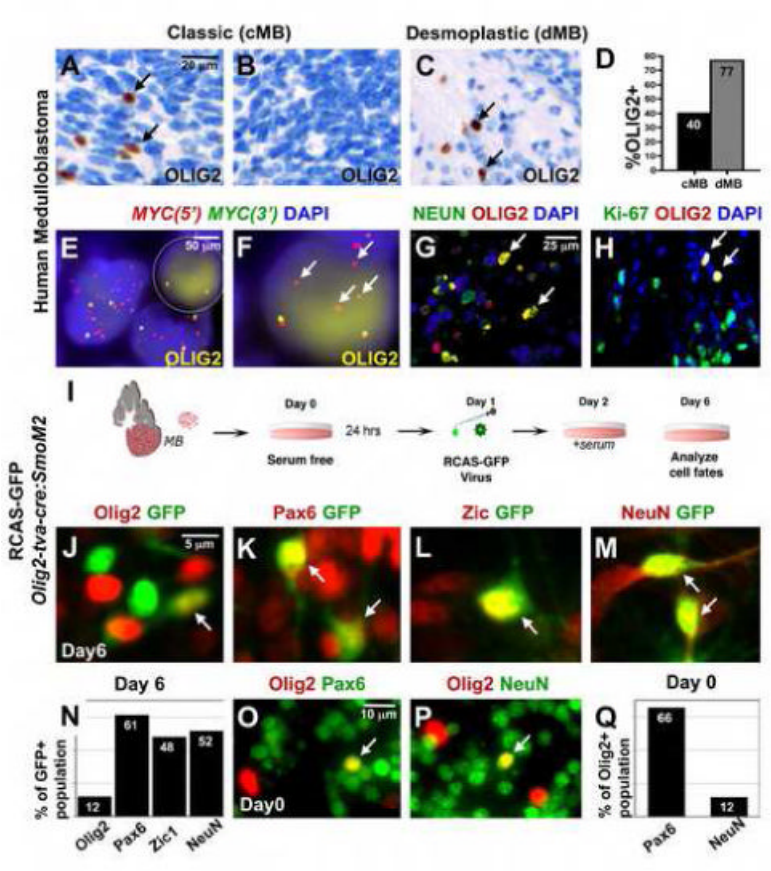

Figure 7. OLIG2 is expressed in human medulloblastoma

(A-D) OLIG2 expression in human classic and desmoplastic MB and percentage of tumors of each class that contain OLIG$^+$ cells (also see Suppl. Tab 1). (E, F) Combined FISH and immunohistochemical analysis reveals the presence of tumor specific *C-MYC* genomic aberrations (Herms et al., 2000) within OLIG2$^+$ cells (yellow nuclei) of human MB (n=2). *C-MYC* aberrations were identical in OLIG2$^+$ and OLIG2$^-$ tumor cells. Note combined copy number gain (red signals, 5′ *C-MYC*) and structural aberration (loss of green signals, 3′ *C-MYC*), as detected using break apart probe set. Normal MYC loci show merged colors as (focal yellow signals). (G, H) OLIG2 co-localizes with NEUN, and the proliferation marker Ki67. (I) Scheme for experiments using RCAS-GFP infection of *Olig2-tva-cre:SmoM2* tumor cells. (J-M) Double-fluorescence images show expression of GFP that co-localizes with immunoreactivity using antibodies against Olig2 and GC lineage markers. Note that while *Olig2-tva-cre:SmoM2* express YFP the signal is very weak/undetectable compared with GFP encoded by RCAS virus, as shown (J-M). (N) Summary of findings at Day 6 in GFP-labeled cells. (O-Q) Analysis of acutely disassociated *Olig2-tva-cre:SmoM2* tumor (Day 0). Of Olig2 + cells, 66% co-labeled with Pax6 and 12% with NeuN, such cells represented 4% and 1% of total cells in the tumor, respectively.

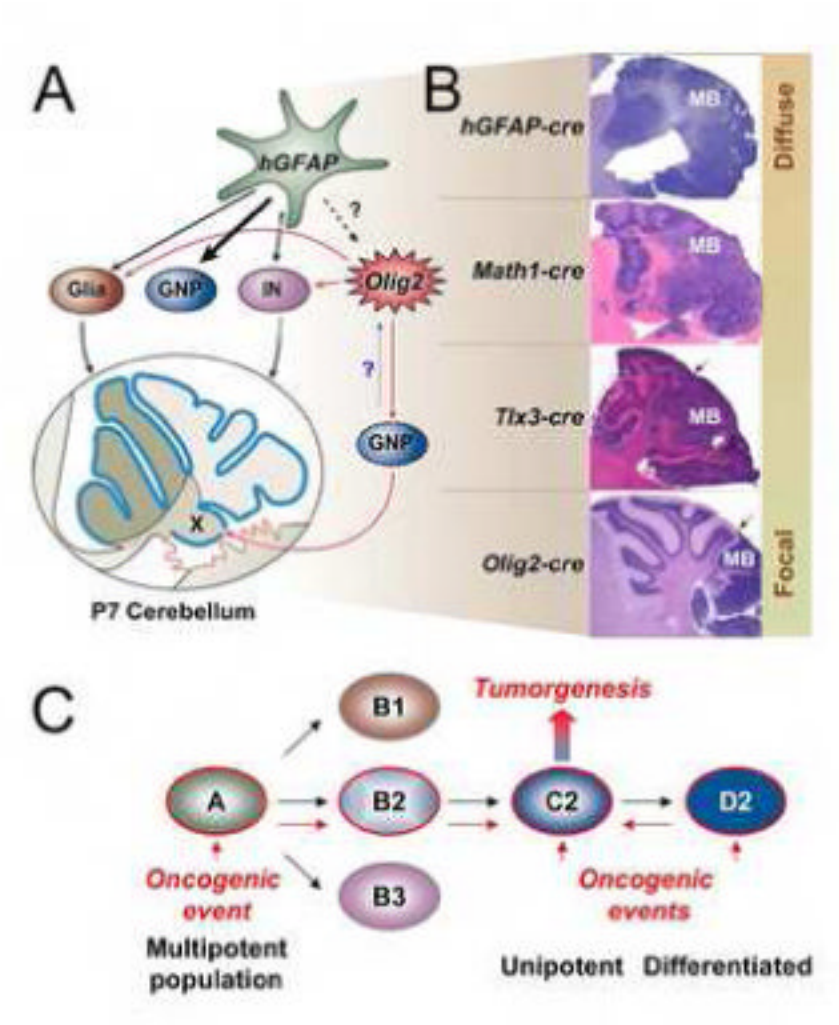

Figure 8. Tumor competent cells of the CGNP lineage can give rise to diffuse and focal forms of medulloblastoma

(A) Scheme showing P7 neuronal progeny deriving from *hGFAP*- and *Olig2*-expressing progenitors of the embryonic CB. *hGFAP*$^+$ cells produce the majority of granule cell precursors (GNP) as well as astrocytes (Glia) and IN. While some *Olig2*$^+$ cells derive from *hGFAP*$^+$ cells (black dashed arrow), additional sources are possible. *Olig2*$^+$ cells of the rRL produce a subset of GNP in cerebellar lobes IX and X, and also give rise to IN and oligodendrocytes (Glia) in all lobes (red arrows). The blue dashed arrow indicates the possibility of GNP de-differentiation in the context of Hh-induced MB. (B) Activation of SmoM2 in GNP using *hGFAP*- or *Math1-cre* produced diffuse MB involving most cerebellar lobes and the vermis, while focal, posterior-lateral MB was produced from the *Olig2-cre* driver; *Tlx3-cre* produced tumors with posterior restriction. (C) Possible cellular pathways of tumorigenesis. Introduction of an oncogene (red arrowheads) into multipotent (A, giving rise to distinct progeny types B1, B2, B3), unipotent (C2) or even differentiated (D2) subtypes of a tumor-competent lineage (e.g., GNP of CB) might result in a uniform tumor phenotype providing only one stage (C2) is capable of rapid expansion in response to the signal. This seems the simplest model to fit our collective findings; however, tumor propagation from an A or B2 cell cannot be ruled out. The later possibility of de-differentiation from D2 > C2 is speculative and not supported by the present work.